Supporting Information

In-Situ Fabricated Gold Nanostars on Hydrogel Beads as Photo-Oxidase Mimic for Rapid and Sustainable POCT of Uric Acid

Tanushree Das, Saurav Das, and Debapratim Das*

Materials

Dipentaerythritol penta-/hexa-acrylate (5ACl), branched polyethylenimine (BPEI), 1-pyrenebutyric acid, 4-(2-Hydroxyethyl)piperazine-1-ethanesulfonic acid (HEPES), and Tetrachloroauric(III) acid ($HAuCl_4$) were purchased from Sigma-Aldrich (USA). 3,3′,5,5′-Tetramethylbenzidine (TMB), 2,2′-azinobis(3-ethylbenzothiazoline-6-sulfonic acid (ABTS), o-Phenylenediamine (OPD), Terephthalic acid (TA), and 3,3′-diaminobenzidine (DAB) were purchased from TCI, Japan. Rink amide MBHA resin, protected as well as unprotected amino acids, and coupling reagents were purchased from Novabiochem. HPLC-grade dimethylformamide (DMF), dichloromethane (DCM) and acetonitrile (ACN) were procured from Spectrochem (India) and Fisher Scientific (India). Solvents were dried whenever required according to the reported procedures. Milli-Q water with a conductivity of less than 2 μScm^{-1} was used for all sample preparations.

Characterization

UV–Visible spectra were recorded on a PerkinElmer Lambda 365+ spectrophotometer, while fluorescence measurements were performed on a Horiba Fluoromax 4 Plus spectrophotometer. The particle sizes of the AuNSs were obtained at 298 K using a 632.8 nm He − Ne laser using Zetasizer Nano- ZS90 (Malvern). FESEM imaging and Energy Dispersive X-ray (EDX) mapping analysis of freeze-dried samples were performed on a Gemini SEM 300 (Sigma Zeiss) instrument. The FETEM analyses were performed in JEOL 2100F microscope. For UV–Visible, FETEM and DLS analysis of the embedded AuNSs (and/or AuNPs), an ethanolic suspension of freeze-dried and ground (henceforth "cryo-ground") AuNS loaded beads was prepared in ethanol through sonication. FTIR spectra for freeze dried samples of the beads were obtained on a PerkinElmer instrument under ambient conditions. The Powder XRD analysis results of the freeze-dried samples were obtained from the Rigaku Smartlab X-ray Spectrophotometer with Cu-Kα (λ =1.54 Å), source running at a power of 9 KW. The TGA analysis was performed in Netzsch, STA449F3A00. Atomic Absorption Spectroscopy was performed using Varian AA240.

Synthesis of PyKC Peptide

The peptide was synthesized on Rink amide MBHA resin using standard Fmoc (9-fluorenylmethoxycarbonyl) solid phase peptide synthesis (SPPS) protocol. In a typical coupling, 3 equiv. of a protected amino acid (with respect to the loading of the resin), 3 equiv. of HBTU, and 6 equiv. of DIPEA were taken in 5 mL of DMF (for 0.1 mmol scale with respect to the resin loading) and stirred for 5 minutes prior to the addition of the mixture to the swelled and deprotected resin. The reaction mixture was shaken for 60 min, and the resin was washed several times with DMF. The Fmoc-deprotection was achieved by treatment of the resin three times with 5 ml of 20% piperidine in DMF for 5 minutes, followed by a thorough washing of the resin with DMF and DCM. The Fmoc-deprotection and coupling steps were repeated until the desired peptide sequence was obtained. The resin with the loaded peptide was washed several times with DMF and DCM and dried. The dried resin

was then treated with a mixture of freshly prepared mixture of 8.5:1:0.5 (trifluoroacetic acid (TFA)/tetraethylsilane (TES)/H_2O) and stirred for 1 h. The resin was finally washed with DCM several times. The cleavage cocktail and the washings combined were concentrated to a minimum volume on a rotary evaporator. The cleaved peptide was then precipitated from cold dry ether, centrifuged and lyophilized to get the crude peptide. Purification was done in Dionex Ultimate 3000 HPLC using a Luna 5 μm (C18) column (Phenomenex) and using acetonitrile and water (containing 0.1% TFA each) as the mobile phase.

^{1}H-NMR (DMSO-d_6, 400 MHz): δ (ppm) 8.39 (d, 1H), 8.28 (m, 2H), 8.23 (m, 2H), 8.14 (d, 2H), 8.07 (t, 1H), 7.97 (t, 2H), 7.66 (s, 3H), 7.29 (s, 1H), 7.20 (s,1H), 4.39 – 4.21 (m, 2H), 2.90 – 2.66 (m, 4H), 2.29 (m, 3H), 2.03 (p, 2H), 1.69 (m, 1H),1.55 (m, 3H), 1.35 (d, 2H).
MALDI-TOF: m/z calculated for $C_{29}H_{34}N_4O_3S$ $[M+H]^+$: 519.27, found: 519.23
HPLC R_T = 12.5 min (HPLC Program: 5% Acetonitrile/Water to 100% Acetonitrile in 20 minutes.)

Preparation of Core-Shell Beads

The core-shells beads were fabricated following our previously reported 2-step protocol.[1]

Step 1: Typically, a 5 wt% solution of PyKC (20 mM Tris buffer, pH 8) was prepared in a 1 mL syringe fitted with a 26G needle and was left undisturbed at room temperature for a period of 24 h to allow the formation of the hydrogel. The hydrogel in the syringe was then forced out through the fine needle orifice using gentle mechanical pressure. Owing to the shear thinning property of PyKC hydrogel, the sol emerging out of the needle immediately hardened into small spherical hydrogel droplets which were dropped into an ethanolic solution of 5ACl (1 g/mL) for surface functionalization. The beads were allowed to react with 5ACl for 15 min with gentle shaking and subsequently washed several times with copious amounts of ethanol to remove the unreacted and loosely bound 5ACl molecules from the surface.

Step 2: The beads, surface-functionalized with acrylate groups, were then treated with an ethanolic solution of BPEI (20 mg/ml) over a shaker for 15 min, followed by washing with ethanol to remove any unreacted BPEI. This led to the cross-linking of the surface of the beads and generated an amine functionalized surface.

Fabrication of Gold Nanostar-Embedded Beads (AuNS@Beads)

The AuNS@Beads were synthesized through a 2-step seeded growth process. Initially, gold nanoseeds were synthesized in situ on the surface of the beads under thermal conditions. Specifically, 20 BPEI-coated beads were continuously agitated in a 1ml aqueous solution of $HAuCl_4$ (100 mM) for 30 minutes at 90 °C, followed by an additional 20 minutes at room temperature. Subsequently, 50 μL of 1M HEPES buffer at pH 7.4 was introduced, and agitation continued for an additional 4 hours. The colour of the solution transitioned from yellow to bluish-green, indicating the formation of gold nanostars, while the

colour of the beads changed from light brown to deep reddish-brown, signifying successful in situ fabrication of gold nanostructures on their surface. The resulting AuNS@Beads were thoroughly rinsed with water to eliminate unreacted reagents and loosely attached nanostars before being stored at 4 °C. Confirmation of AuNS formation within the BPEI polymeric shell was achieved through various analyses including UV-Visible, DLS, and FETEM.

Fabrication of Gold Nanoparticles-Embedded Beads (AuNP@Beads)

The AuNP@Beads were synthesized under thermal conditions following a previously established protocol.[1] Specifically, 15 BPEI-functionalized beads were continuously agitated in a 1ml aqueous solution of $HAuCl_4$ (100 mM) for 3 hours at 90 °C. Subsequently, the resulting AuNP@Beads were thoroughly rinsed with water to eliminate unreacted reagents and loosely attached nanoparticles. The AuNP@Beads were then stored at 4°C until further use. Confirmation of AuNP formation within the BPEI polymeric shell was attained through various analyses including UV-Visible and FETEM examinations.

Assessment of Oxidase-Like Activity

The oxidase activity of the AuNS@Beads was evaluated by spectrophotometrically monitoring the oxidation process of the chromogenic substrate, TMB. In a typical procedure, 0.5 mM TMB (1 µL of 0.5 M stock solution in DMSO) was taken in 1 mL of pH 7 phosphate buffer (20 mM) in a quartz cuvette with a path length of 1 cm. To initiate the reaction, one AuNS@Bead was inserted into the cuvette, the solution was thoroughly mixed, and the solution was exposed to visible light irradiation (20 W white-light LED bulb; $\lambda \geq 420$ nm). UV-Visible spectra of the solution were recorded at 2-minute intervals for a duration of 20 minutes. The gradual emergence of an absorbance band at 652 nm, corresponding to the charge-transfer complex of oxidized-TMB, provided evidence for the oxidase activity of the AuNS@Beads. Similarly, the oxidation of ABTS and OPD (0.5 mM each) by the AuNS@Beads further confirmed the oxidase activity of the gold nanostars.

Assessment of pH Dependent Oxidase-Like Activity

The pH-dependent oxidase activity of AuNS@Beads was assessed by spectrophotometrically monitoring the oxidation of TMB across various buffers ranging from pH 2 to pH 8 (20 mM). In a typical procedure, 0.5 mM TMB (1 µL from a 0.5 M stock solution in DMSO) was dissolved in 1 mL of the corresponding buffer solution in a quartz cuvette with a 1 cm path length. The reaction was initiated by adding a single AuNS@Bead into the cuvette, followed by thorough mixing. After a 10-minute incubation period under visible light irradiation, UV-Visible spectra of the solutions were recorded. Catalysis experiments were conducted in triplicate, and the intensity of the absorption spectra at 652 nm was utilized to evaluate the relative oxidase activity of the AuNS@Beads under varying pH conditions.

Kinetic Analysis of the Oxidase-Like Catalysis

The oxidase activity of AuNS@Beads under visible light irradiation and in the absence of light at pH 5 was evaluated by spectrophotometrically monitoring the oxidation of TMB. In brief, a single AuNS@Bead was placed in 1 mL of pH 5 acetate buffer (20 mM) within a quartz cuvette of 1 cm path length and varying amounts of TMB (1 µL of 0.2, 0.4, 0.6, 0.8, and 1.0 M stock solutions in DMSO used to attain final concentrations of 0.2, 0.4, 0.6, 0.8, and 1.0 mM, respectively) were added to the solution. Following mixing, the solutions were allowed to sit in darkness or exposed to visible light for five minutes. After that, the absorbance of the oxidized TMB charge-transfer complex at λ_{max} = 652 nm (with $\varepsilon_{652\ nm}$ = 39000 $M^{-1}.cm^{-1}$ in water) was measured. Catalysis experiments were conducted in triplicate, and the kinetics of the reactions at different pH values were determined via nonlinear regression using GraphPad Prism 9 software, assuming Michaelis-Menten kinetics.

Band Gap Analysis of AuNS/AuNP

The band gap was extracted by converting the UV-visible spectral data into a Tauc plot using Tauc's equation[2] for direct band gap materials:

$$(\alpha h\vartheta)^2 = k(h\vartheta - E_g) \quad \text{S1}$$

where α is the absorption constant, hυ is the photon energy, E_g is the band gap energy, and k is a constant. This equation can also be expressed as

$$(2.303 \times A \times \frac{1240}{\lambda})^2 = k(\frac{1240}{\lambda} - E_g) \quad \text{S2}$$

where A represents absorbance and λ is the wavelength derived from the UV-Visible spectra of the AuNS and AuNP. Plotting this equation results in a graph (Fig. S9B), where. the tangent of the curve corresponds to the band gap energy of the AuNS and AuNP.

ROS Scavenger Study

To investigate the generation of various reactive oxygen species (ROS) within the system, a ROS scavenger study was conducted. In this experiment, a single AuNS@Bead was incubated with different scavengers (1 mM NaN_3, 0.4 mM histidine, 10 mM BQ, 10 mM IPA, 20 mM t-BuOH, 5 mM KI, and 1 mM EDTA) in 1 mL of pH 5 acetate buffer under visible light irradiation for 30 minutes. Subsequently, 0.5 mM TMB was introduced into the solution, followed by further incubation for 5 minutes. The UV-Visible spectrum was then recorded to assess the impact of the scavengers on the oxidation reaction.

3,3′-Diaminobenzidine (DAB) Assay

3,3′-diaminobenzidine (DAB) serves as a probe for detecting singlet oxygen generation in aqueous systems. To assess the production of singlet oxygen, 1 mM DAB was introduced into a 1 ml solution of pH 5 acetate buffer (20 mM) containing one AuNS@Bead, and DAB oxidation was monitored by

UV-Visible spectrophotometry at fixed time intervals under both light and dark conditions. In order to assess the impact of photogenerated holes and superoxide radicals on the process of generating singlet oxygen, DAB oxidation was also observed in the presence of 5 mM KI (positive holes scavenger) and 10 mM BQ (superoxide radical scavenger).

Terephthalic Acid (TA) Assay

Terephthalic acid acts as a probe to capture hydroxyl radicals, leading to the formation of a highly fluorescent product known as 2-hydroxyterephthalic acid. In this experiment, a solution containing 0.5 mM TA in 1 mL of pH 5 acetate buffer (20 mM) was subjected to a one-hour incubation period under light irradiation, in the presence of H_2O_2, AuNS@Bead, and a combination of both. Following incubation, the fluorescence spectra of the solutions were monitored at 435 nm using an excitation wavelength of 315 nm. The absence of a prominent emission band at 435 nm in presence of AuNS@Bead and H_2O_2 indicates that the system does not generate hydroxyl radicals.

Assessment of Superoxide Dismutase (SOD)-Like Activity

To evaluate the SOD-like activity of AuNS@Beads, the generation of H_2O_2 was indirectly analysed by spectrophotometrically monitoring the oxidation of the chromogenic substrate TMB by HRP, utilizing the H_2O_2 produced through SOD catalysis. In this assay, a single AuNS@Bead was incubated with 0.4 mM histidine in 1 mL of pH 5 acetate buffer under visible light irradiation for 30 minutes. Following this, 0.5 mM TMB and 10 units/mL HRP was added to the solution, and the mixture was incubated for an additional 5 minutes. The UV-Visible spectrum was then recorded to determine H_2O_2 generation via SOD catalysis. In this setup, histidine acts as a scavenger for singlet oxygen, preventing TMB oxidation via oxidase catalysis.

Colorimetric Detection of Uric Acid

Initially, a solution containing 0.5 mM TMB in 1 mL of pH 5 acetate buffer (20 mM) was subjected to oxidation by a single AuNS@Bead under light irradiation for a duration of 30 minutes. Following this, the bead was extracted using a pair of forceps, and incremental concentrations of uric acid were introduced into the coloured oxidized-TMB solution. The change in the colour of the solution upon each successive addition of uric acid was monitored via UV-Visible spectrophotometry. The absorbance difference, ΔA_{652nm} (the difference in absorption intensity at 652 nm before and after the uric acid addition), served as the basis for constructing the calibration curve and facilitated the determination of uric acid concentrations.

Smartphone-Assisted Detection of Uric Acid

In a vial, a solution containing 0.5 mM of TMB in pH 5 acetate buffer (20 mM) was oxidised by a single AuNS@Bead under light irradiation for 30 minutes. Subsequently, the bead was carefully removed,

and a 100 µL aliquot of the oxidized-TMB solution was transferred to an inverted vial cap with a diameter of 0.5 cm. This vial cap was positioned within a self-constructed sample chamber measuring 20 cm (L) x 15 cm (W) x 10 cm (H). A digital image of the coloured solution was captured using a smartphone camera, positioned 10 cm away from the sample, with illumination provided by the smartphone's LED flashlight. Following this, increasing concentrations of uric acid were added to the oxidized-TMB solution in the vial. Following each addition, a 100 µL aliquot of the solution was isolated, and its digital image was recorded. All captured images were analysed using the "Color Picker" app and processed to determine the R, G, and B parameters. The colour intensities of the samples were calculated using the formula, $I = 0.3R + 0.59G + 0.11B$, where I represents intensity. The difference in intensity of the oxidized-TMB solution before and after the addition of uric acid, denoted as ΔI, was utilized to establish the calibration curve, enabling the precise determination of uric acid concentrations.

For assessing the uric acid content in real samples, two 90 µL aliquots of the oxidized-TMB solution were dispensed into separate inverted vial caps, each with a diameter of 0.5 cm. To one of these aliquots, 10 µL of the uric acid sample (either undiluted blood serum or five-fold diluted urine) was added, while the other aliquot received 10 µL of pH 5 acetate buffer. Subsequently, the colour intensities of the two aliquots were measured using a smartphone camera, and the concentration of uric acid in the samples was determined by referencing the obtained intensities to the calibration curve previously established. The blood and urine samples were obtained from donors with written consent and no ethics committee approval was necessary for these samples.

FTIR Analysis of surface functionalisation

Functionalization of the bead surface with 5ACl followed by BPEI was ascertained through FTIR spectroscopy of the freeze-dried beads after subsequent functionalization steps (Figure S1). Appearance of new peaks at 1408 and 1735 cm^{-1} corresponding to the asymmetric stretching vibration of the vinyl group and stretching vibration of ester carbonyl groups, respectively, affirmed the successful attachment of 5ACl on the surface of the peptide hydrogel beads.[1] As the peptide amide bonds remain unaffected during surface functionalization, taking the amide carbonyl stretching band at 1635 cm^{-1} as an internal standard, a relative decrease in the amine stretching band at 1540 cm^{-1} following 5ACl functionalization indicated the free lysine amine groups on the surface of the beads underwent Michael addition reaction with the 5ACl molecules. Also, as the ester groups of 5ACl do not participate in subsequent functionalization reaction, a relative decrease in the peak intensity at 1408 cm^{-1} for C-H stretching of the vinyl groups compared to the carbonyl stretching of 5ACl ester groups at 1735 cm^{-1} indicated the Michael addition of BPEI with the residual 5ACl acrylate moieties on the bead surface.

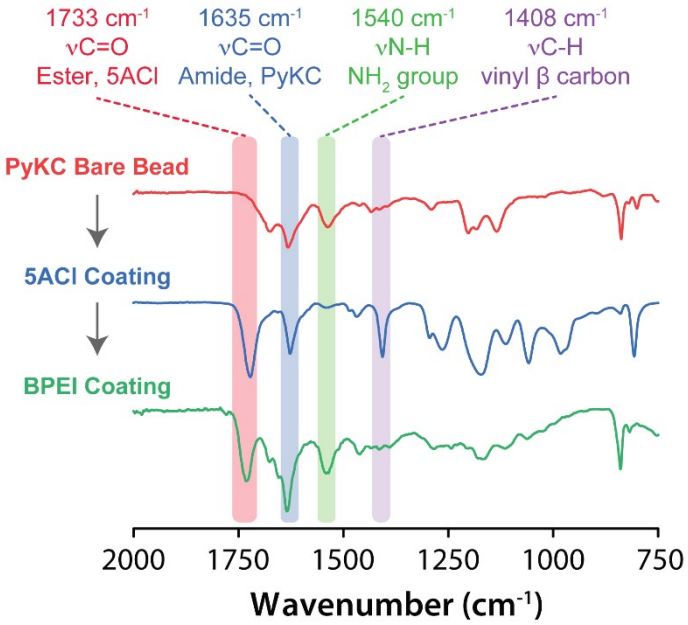

Figure S1. FTIR spectra of the beads after each successive surface modification step

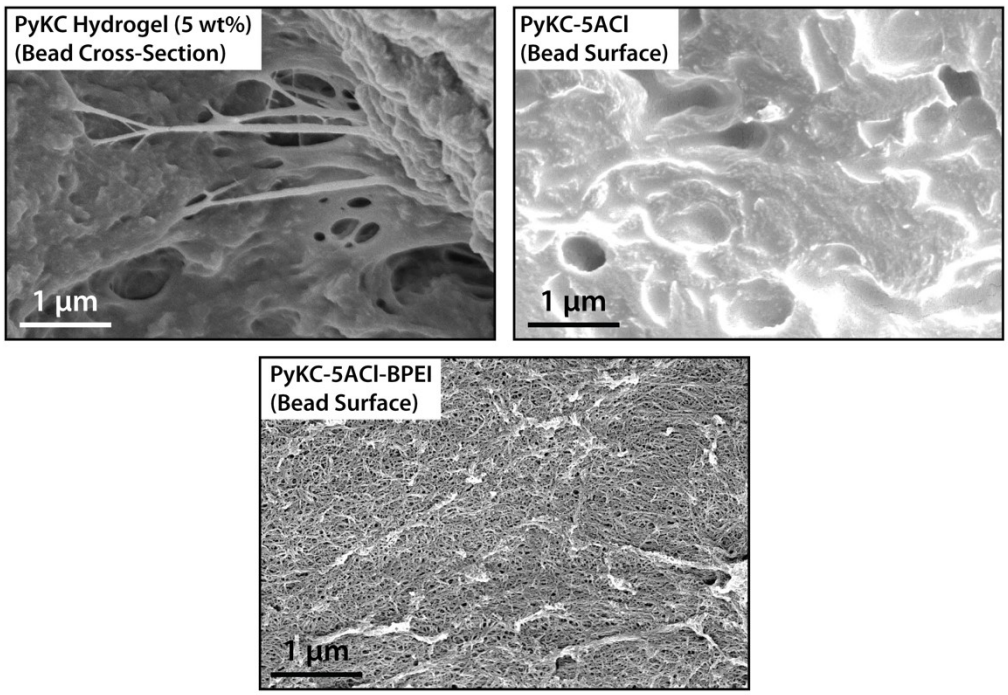

Figure S2. FESEM images of the bead surface after each successive surface modification step

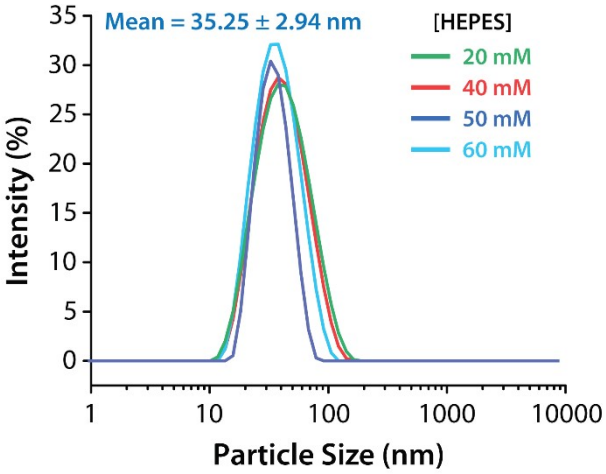

Figure S3. Representative plot of the DLS profile of the in-situ synthesized AuNSs

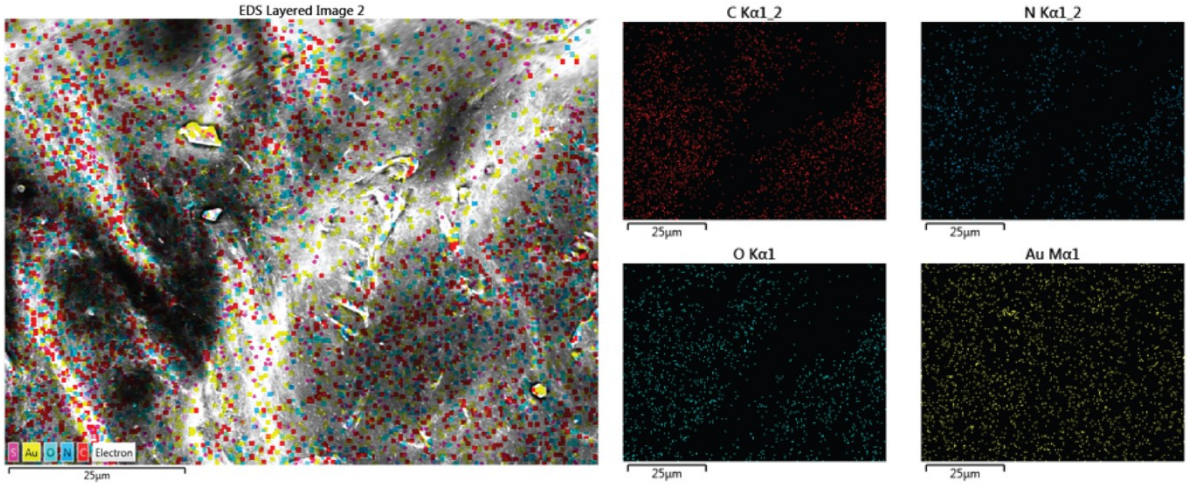

Figure S4. EDX elemental mapping of the surface of the AuNS embedded bead

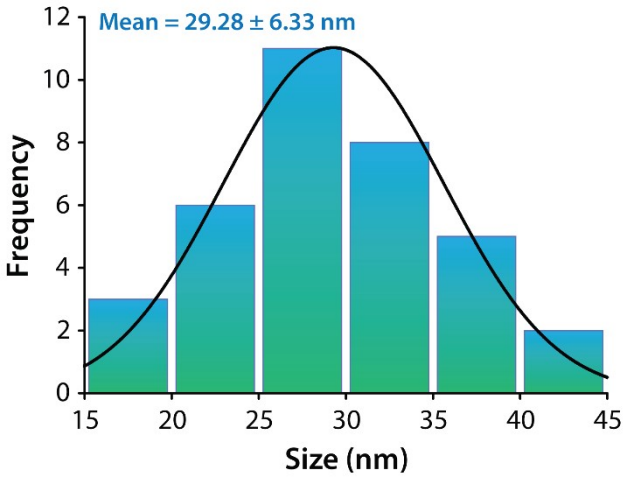

Figure S5. Size distribution histogram of the in situ synthesized AuNSs

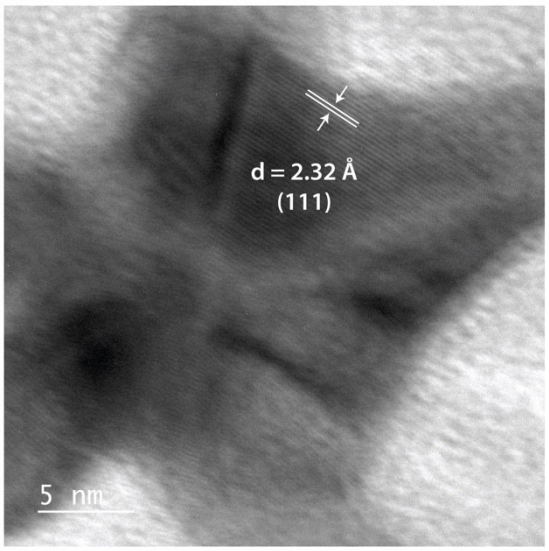

Figure S6. HRTEM image of the in-situ synthesized AuNS

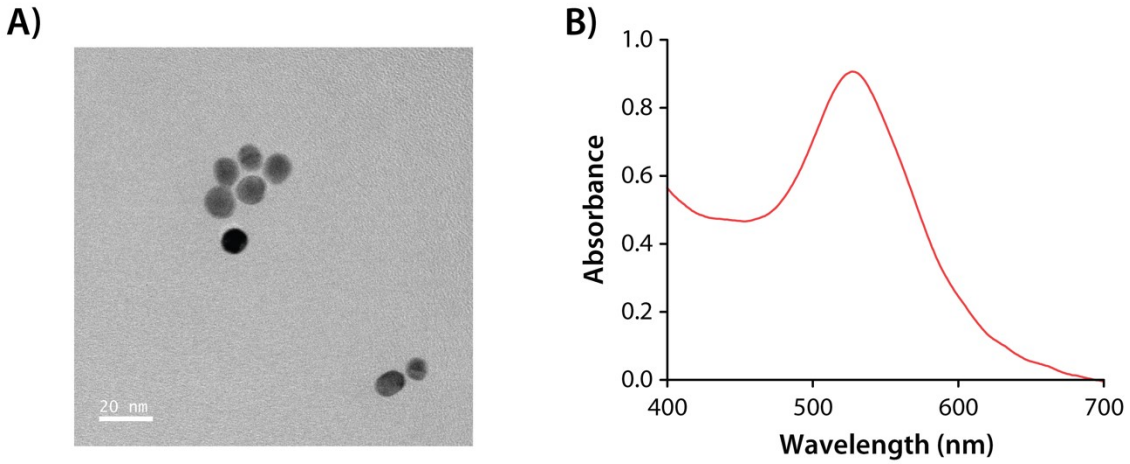

Figure S7. A) FETEM image, and B) UV-Visible spectrum of cryo-ground ethanolic suspension of AuNP@Beads

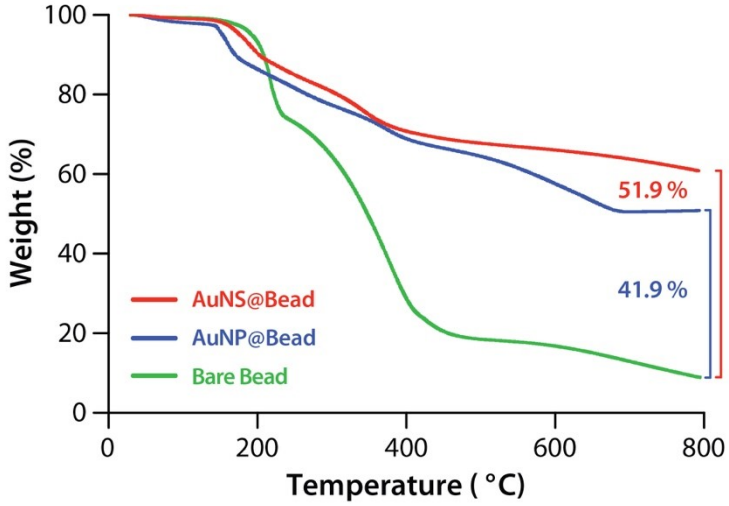

Figure S8. TGA profiles of the bare, AuNS-embedded, and AuNP-embedded core shell beads

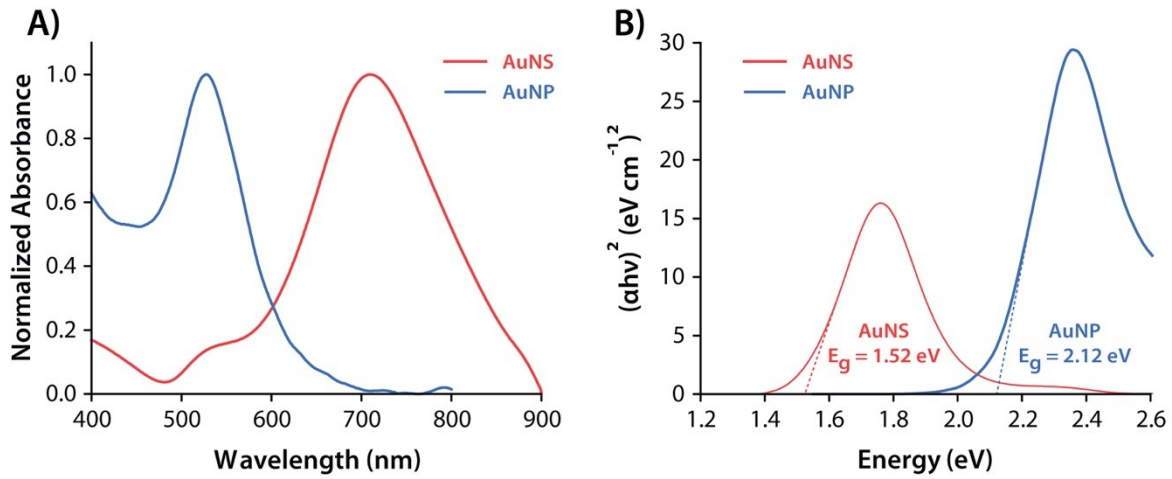

Figure S9. A) Normalized UV-Visible spectra, and B) Tauc's plot for the band gap energy of the AuNS and AuNP

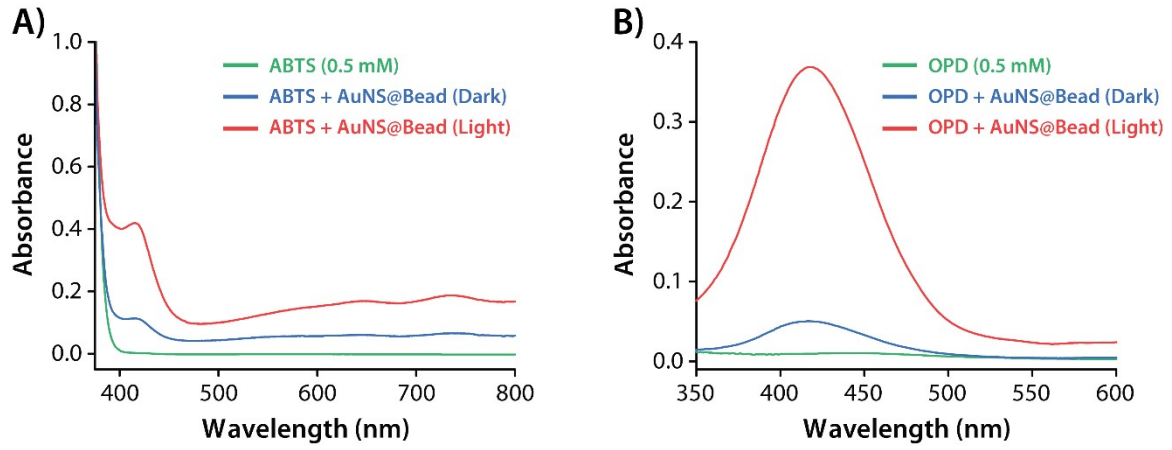

Figure S10. UV-Visible spectra showing light-activated photo-oxidation of A) ABTS, and B) OPD, by the AuNS@Beads

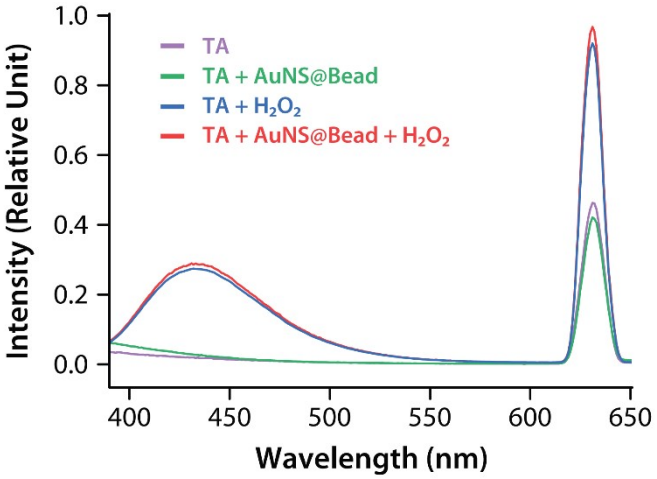

Figure S11. Fluorescence spectra of the TA assay for detecting hydroxyl radicals

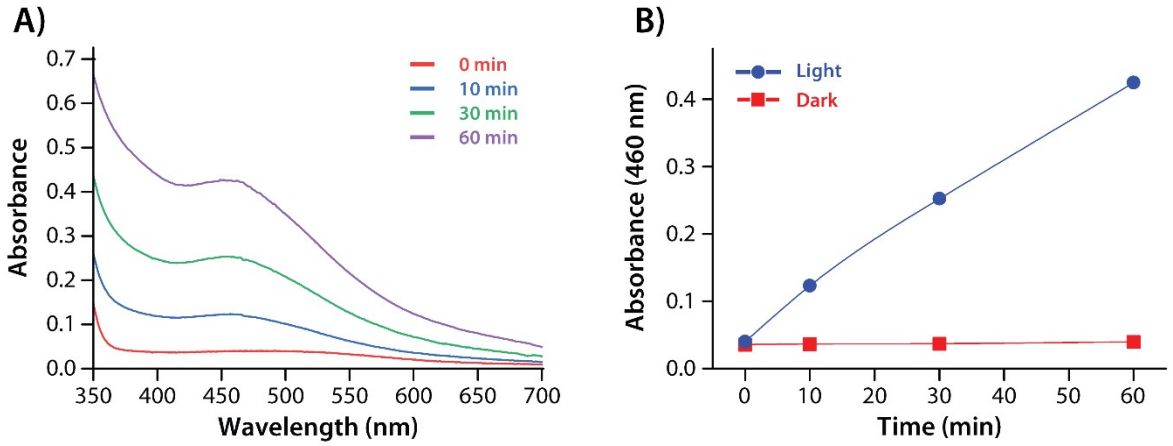

Figure S12. A) UV-Visible spectra of the DAB assay for detecting singlet oxygen, and B) Comparison of the DAB assay under light and dark conditions.

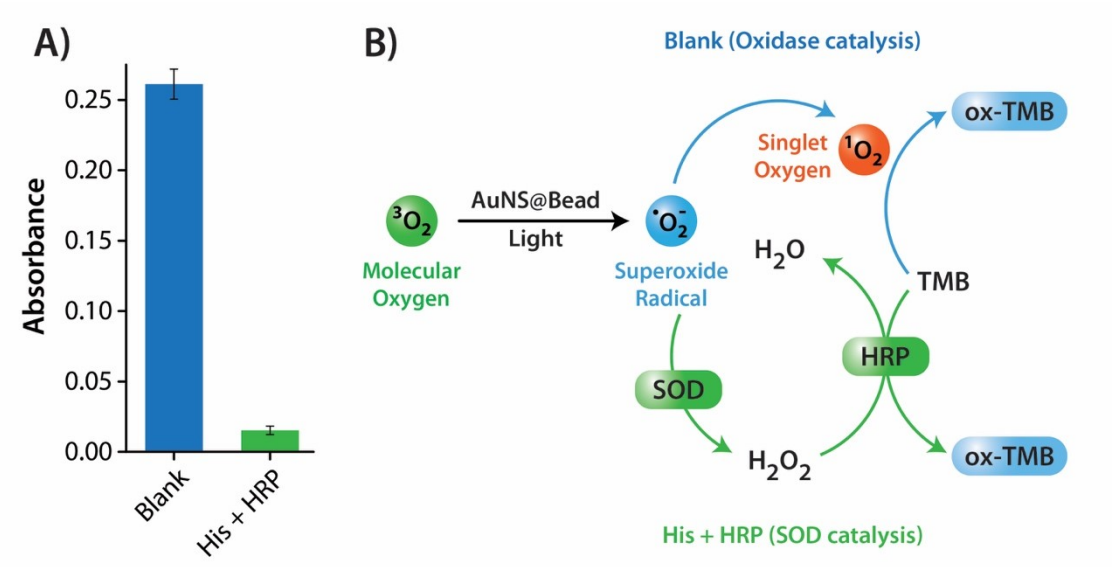

Figure S13. A) Comparison of absorbance intensity of oxidised-TMB charge-transfer complex at 652 nm upon oxidation of TMB through photo-oxidase catalysis (Blank) and peroxidase catalysis by HRP using H_2O_2 generated via SOD catalysis (His + HRP). B) Schematics showing the oxidation of TMB via oxidase catalysis, and SOD catalysis.

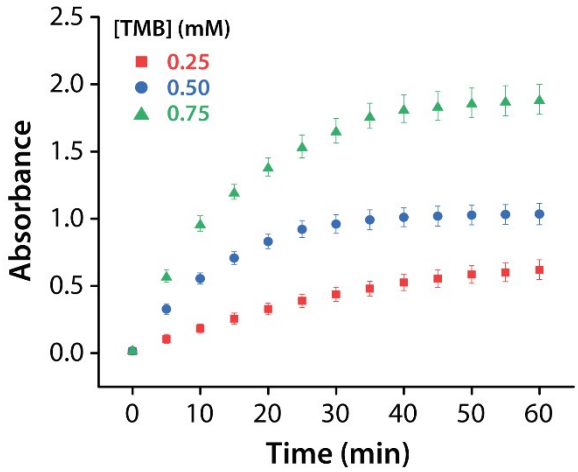

Figure S14. Time-dependent change in the absorbance of oxidised-TMB charge-transfer complex at 652 nm during photo-oxidation across varying concentrations of TMB substrate

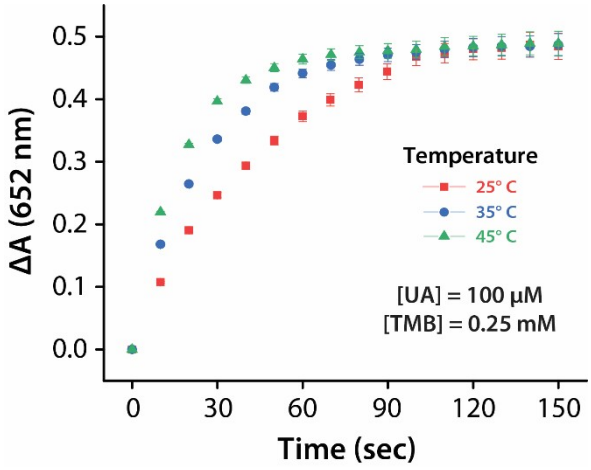

Figure S15. Time-dependent variation in the absorbance intensity of oxidized TMB charge-transfer complex at 652 nm following the addition of uric acid at varying temperatures

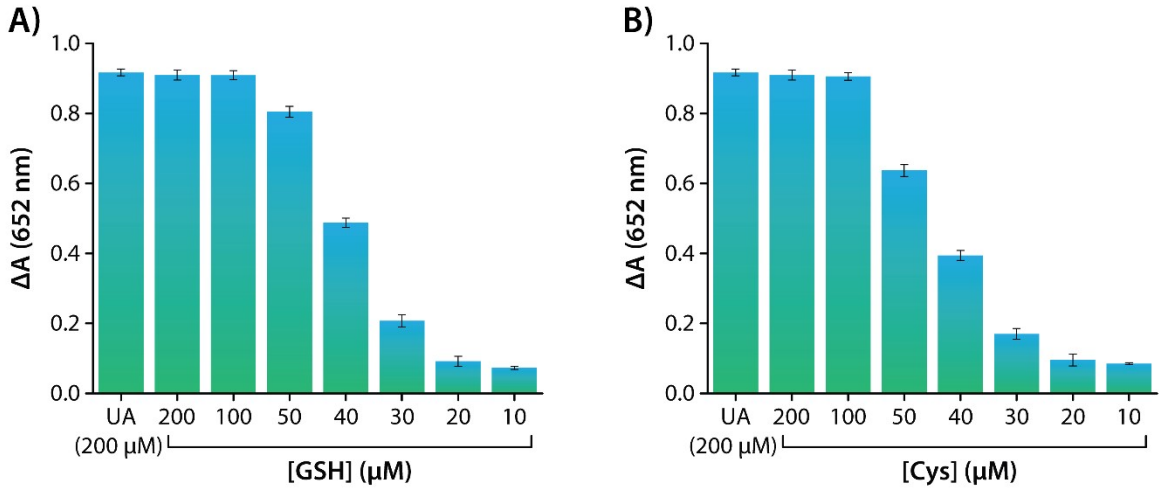

Figure S16. Comparison of change in absorbance intensity of oxidised-TMB charge-transfer complex at 652 nm upon addition of varying concentrations of A) GSH, and B) L-Cysteine

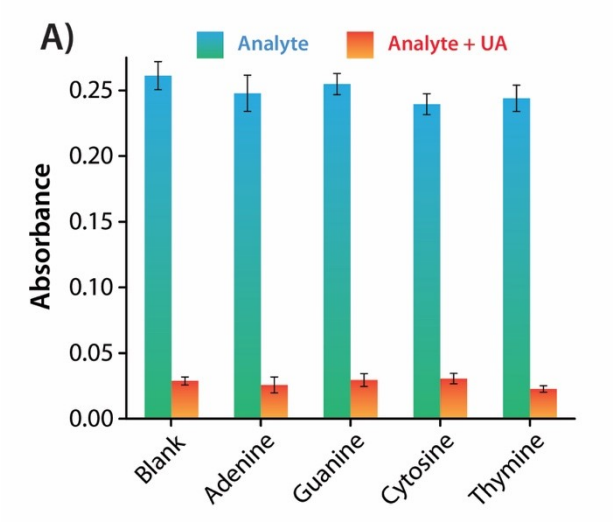

Figure S17. Comparison of absorbance intensity of oxidised-TMB charge-transfer complex at 652 nm upon addition of various purine and pyrimidine bases, both in the absence and presence of uric acid. [TMB] = 0.5 mM, [UA] = 200 µM, Concentration of the analytes = 500 µM

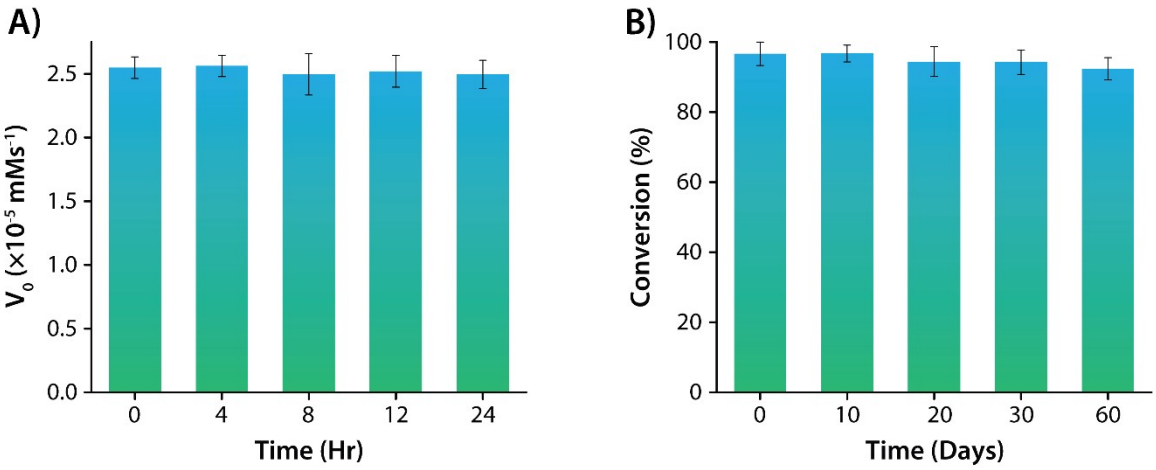

Figure S18. Catalytic activity of AuNS@Beads at different time intervals of continuous agitation in water

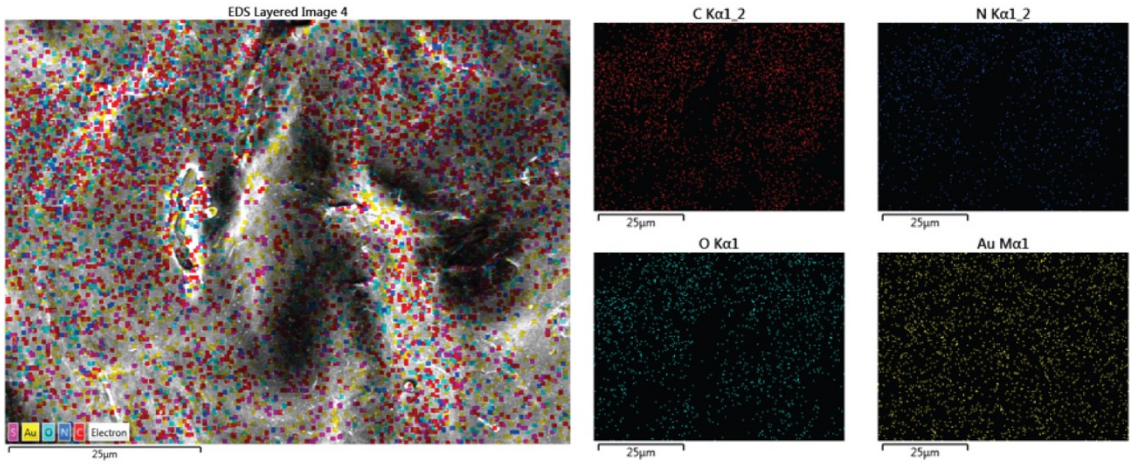

Figure S19. EDX elemental mapping of the surface of the AuNS embedded bead after catalytic cycles

Table S1. Comparison of catalytic performance of previously reported catalytic materials for the sensing of uric acid

Material	Linear Range (µM)	LOD (µM)	Reference
Histidine-doped porphyrin covalent organic framework nanozyme	5-100	5	[3]
Upconversion-nanoparticle-functionalized janus micromotors	100-5000	1.59	[4]
Hemin-graphene oxide (H-GO)/Uricase-based photoacoustic device	100-2000	36	[5]
Hemin-functionalized microfluidic chip	1-1000	0.41	[6]
MXene-$Ti_3C_2T_x$ based electrochemical microfluidic biosensor	30-500	5	[7]
Prussian blue nanoparticles	0.5-50	0.9	[8]
TABB-BDB COF	29.74–951.76	21.24	[9]
Gold nanostars embedded hydrogel beads	10-200	0.9	This work

Table S2. Determination of uric acid content in blood serum and urine samples using spectrophotometric and POCT-based methods. Blood samples are diluted 10 times while the urine samples are diluted 50 times.

Sample No.	Pathology Lab Determined (μM)[a]	Uric Acid Added (μM)	Spectrometric Determination (μM)	Recovery (%)	RSD (%, n=3)	POCT Determination (μM)	Recovery (%)	RSD (%, n=3)
Sample **1**[b] Blood Serum	327.2	0	33.1 ± 0.9	-	2.8	32.3 ± 1.0	-	3.2
		10	43.9 ± 1.4	101.8	3.1	43.4 ± 1.2	102.6	2.8
		30	61.9 ± 1.3	98.1	2.1	63.1 ± 1.8	101.3	2.9
		50	81.3 ± 2.0	97.8	2.5	80.9 ± 1.7	98.3	2.1
Sample **2**[b] Blood Serum	345.0	0	33.5 ± 1.1	-	3.2	33.8 ± 0.9	-	2.8
		10	43.3 ± 1.2	97.4	2.8	43.5 ± 1.3	99.3	3.1
		30	65.3 ± 1.4	101.3	2.1	64.8 ± 1.7	101.5	2.6
		50	86.3 ± 2.5	102.1	2.9	86.1 ± 2.3	102.7	2.7
Sample **3**[c] Urine	-	0	50.8 ± 1.4	-	2.7	49.9 ± 1.2	-	2.5
		10	60.0 ± 1.1	98.7	1.9	58.3 ± 1.8	97.3	3.1
		30	78.5 ± 1.6	97.2	2.1	78.5 ± 2.2	98.2	2.8
		50	103.2 ± 2.4	102.4	2.3	101.3 ± 1.9	101.4	1.9
Sample **4**[c] Urine	-	0	74.5 ± 1.3	-	1.8	76.7 ± 1.6	-	2.1
		10	83.3 ± 1.9	98.6	2.3	88.1 ± 2.4	101.6	2.7
		30	101.6 ± 2.1	97.2	2.1	104.9 ± 3.1	98.3	3.0
		50	126.6 ± 2.4	101.7	1.9	129.7 ± 3.2	102.4	2.5

[a] Data supported by the affiliated hospital of IIT Guwahati; [b] 10-fold diluted sample; [c] 50-fold diluted sample.

References

1. T. Das, S. Das and D. Das, *Chem. Eng. J.*, 2023, **477**, 147105.
2. A. C. Ekennia, D. N. Uduagwu, N. N. Nwaji, O. O. Oje, C. O. Emma-Uba, S. I. Mgbii, O. J. Olowo and O. L. Nwanji, *J. Inorg. Organomet. Polym. Mater.*, 2021, **31**, 886-897.
3. C. Zhong, C. Hu, D. Ouyang, A. Dan, Y. Zhong, Z. Cai and Z. Lin, *Chem. Eng. J.*, 2023, **477**, 146979.
4. P. Zhao, Y. Liu, Y. Chen, M. Yang, S. Zhao, N. Qi, Y. Wang, D. Huo and C. Hou, *ACS Appl. Mater. Interfaces*, 2022, **14**, 41369-41378.
5. Y.-J. Zhang, L. Guo, Y.-L. Yu and J.-H. Wang, *Anal. Chem.*, 2020, **92**, 15699-15704.
6. P. Zhao, Y. Liu, Y. Chen, M. Yang, S. Zhao, N. Qi, Y. Wang, D. Huo and C. Hou, *ACS Appl. Mater. Interfaces.*, 2022, **14**, 41369-41378.
7. J. Liu, X. Jiang, R. Zhang, Y. Zhang, L. Wu, W. Lu, J. Li, Y. Li and H. Zhang, *Adv. Funct. Mater.*, 2019, **29**, 1807326.
8. B. Hou, X. Guo, Y. Zhang, L. Zhang, D. Zhang, Z. Wu, J. Zhang and Z. Hao, *ACS Sustain. Chem. Eng.*, 2023, **11**, 6211-6219.
9. C.-X. Liu, Z.-W. Zhou, Y. Yu, Y.-J. Wei, C.-X. Cai, N. Wang and X.-Q. Yu, *Small Struct.*, 2023, **4**, 2200321.